

# Coronal and chromospheric emission from cool stars in near-simultaneous ROSAT all-sky survey and Mount Wilson data<sup>★</sup>

A.J.M. Pijters<sup>1</sup>, C.J. Schrijver<sup>2</sup>, J.H.M.M. Schmitt<sup>3</sup>, C. Rosso<sup>3</sup>, S.L. Baliunas<sup>4</sup>, J. van Paradijs<sup>1,5</sup>, and C. Zwaan<sup>2</sup>

<sup>1</sup> Astronomical Institute ‘Anton Pannekoek’ / CHEAF, Kruislaan 403, 1098 SJ Amsterdam, The Netherlands

<sup>2</sup> Astronomical Institute, Postbus 80.000, 3508 TA Utrecht, The Netherlands

<sup>3</sup> Max Planck Institut für Extraterrestrische Physik, Giessenbachstraße, D-8046 Garching bei München, Germany

<sup>4</sup> Centre for Astrophysics, 60 Garden Street, Cambridge, MA 02138, USA

<sup>5</sup> Physics Department UAH, Huntsville, AL 35899, USA

Received 29 May 1995 / Accepted 18 March 1997

**Abstract.** Mt. Wilson Ca II H&K line-core emission fluxes for 215 F-, G- and K-type stars were obtained within at most a few days of the corresponding ROSAT All-Sky Survey observations. These stars cover wide ranges of stellar activity, spectral type and luminosity class. In this paper we study the well-known relationship between the Ca II H&K line-core emission in excess of the minimum emission and the soft X-ray emission. We find that flux densities normalised with the bolometric flux densities are the best quantity in which to express activity when comparing radiative emission in different temperature regimes. We find a power-law relationship, in which the X-ray normalised emission varies approximately quadratically with the normalised excess Ca II H&K line-core emission. This relationship does not depend on luminosity class at least up to luminosity class III, and it does not depend on effective temperature. The scatter around this relationship is consistent with the measurement errors. The X-ray spectral hardness ratios of main-sequence stars increase with the X-ray flux densities; a similar trend, but with substantially larger scatter, is also present for evolved stars. A comparison between values from different passbands of the Mt. Wilson HK spectrophotometer shows that relatively hot stars ( $(B - V) \leq 0.50$ ) appear to have a Ca II line core emission peak about a factor 2 to 3 wider than cooler stars.

**Key words:** stars: activity – stars: chromospheres – stars: coronae – stars: late-type – X-rays: stars

## 1. Introduction

Stars with spectral types later than approximately mid-F, and possibly as early as  $\sim A7$ , show signs of magnetic surface activity, accompanied by an outward temperature increase in their

outer atmospheres. The amounts of radiation originating from different temperature intervals in these outer atmospheres (i.e., the chromosphere, the corona, and the transition region between these two) have been used to measure this magnetic activity; well-known examples are the chromospheric Ca II H&K line core emission and the coronal X-ray emission (for reviews see Zwaan 1991, and Vaiana 1983).

Several studies (e.g., Rutten et al. 1991, Zwaan 1991, and references therein) have shown that chromospheric and coronal emissions are strongly correlated for stars with spectral types from mid F to mid K. Main-sequence stars and evolved stars follow the same relationship between the stellar surface fluxes emitted in X-rays and in the Ca II H&K line cores, independent of spectral type, provided that a minimum flux density (which depends on spectral type, and perhaps weakly on luminosity class) is subtracted from the observed value.

Rutten et al. (1991) showed that the power-law index of a flux-flux relation increases with the difference between the formation temperatures of the two radiative diagnostics. Schrijver (1993) argues that the non-linearity of the stellar Ca II – X-ray relationship is caused by the non-linear dependence of Ca II K line-core emission on the mean magnetic flux density, as observed in solar active regions (Schrijver et al. 1989) and seen in model calculations by, e.g., Solanki et al. (1991), while the X-ray flux density is proportional to the magnetic flux density (Schrijver et al. 1987).

Studies on flux-flux relationships all result in the same quantitative description of these relationships, but they differ significantly on qualitative aspects as, e.g., which unit of radiative emission is best describing the flux-flux relationships; is there *one* flux-flux relation for *all* (‘normal’) magnetically active stars (from late A to M and from giants to dwarfs); what is the power-law index of the relationship (*when* the relationship can be expressed as a power-law)? The main reason why these studies do not give the same results is that the samples of stars used have not been the same and have been rather small (a few tens of stars).

*Send offprint requests to:* J. van Paradijs

<sup>★</sup> Tables 1 and 2 are only available in electronic form at the CDS via anonymous ftp to cdsarc.u-strasbg.fr (130.79.128.5) or via <http://cdsweb.u-strasbg.fr/Abstract.html>

In order to verify the general validity of the relation between the variable coronal and chromospheric fluxes, independent of effective temperature and surface gravity, and in order to answer the questions stated above, it is necessary to derive this relation as accurately as possible for a large sample of stars. This is the first topic addressed in this paper.

Another question concerns the effect of variability on time scales larger than about one day on the scatter about the average relationship. Schrijver et al. (1992) found that the flux-flux relations between chromospheric and coronal diagnostics derived until then showed no deviations other than measurement uncertainties when the fluxes are observed with time intervals of only a few days or less. This was based on a small sample of 20 F6–K2 dwarfs and giants. With more accurate observations and a much larger sample of stars the contribution of variations in magnetic structure in the observed atmosphere to the remaining scatter can be studied. The deviation of an individual star from the mean X-ray vs. Ca II relationship is expected to depend on the time difference between the measurements.

The ROSAT All-Sky Survey, which was conducted from July 1990 until January 1991, offered an opportunity to determine the relationship between the X-ray and Ca II emission for a sizable sample of stars. We obtained Ca II H&K line photometry for 215 F-, G- and K-type stars at the Mt. Wilson Observatory at times as close as possible (mostly within a few days) to the ROSAT All-Sky Survey observation times. In Sect. 2 we discuss the observations and data reduction of the Ca II photometry, and of the X-ray measurements. Flux densities are derived in Sect. 3. The relationship between the stellar flux densities in X-rays and in the Ca II H&K lines is derived in Sect. 4. In Sect. 5 we discuss our results and compare them with previous work. Our conclusions are presented in Sect. 6.

## 2. The data

### 2.1. Ca II H&K photometry

We have obtained Ca II H&K line photometry of 215 stars at the Mt. Wilson Observatory; most of the stars were observed within a few days of the scanning of these stars in the ROSAT All-Sky Survey. For only 9 stars the Ca II observations were separated by more than three weeks from the time of the All-Sky Survey observation.

The stars have been selected from the sample of Rutten (1987a), and are listed in Table 1. They are F-, G- and K-type stars of luminosity classes II to V, with known rotation rate. The sample stars are distributed over a large range in  $B - V$  (0.4–1.5) and rotation period (1–400 days).

The Mt. Wilson H&K spectrophotometer measures the flux in two windows with 1Å or 2Å FWHM centered on the Ca II H&K line cores, and in two 20Å FWHM reference windows located on either side of the H&K doublet. The line-core emission index  $S$  is defined as the ratio between the number of counts in the line-core windows and the number of counts in the reference windows, scaled with a normalisation constant. A detailed description of the photome-

ter and of the measurement procedure has been given by Vaughan et al. (1978). For most dwarfs and subgiants (luminosity classes IV to V) the 1Å FWHM passband ( $S_1$ -value) was used; for most giants and bright giants (luminosity classes II to III-IV) the 2Å FWHM passband ( $S_2$ -value) was used to accommodate their broader emission profiles in the H&K line cores (Wilson and Bappu 1957). Exceptions have been indicated in Table 1.

For most stars the Ca II H+K line-core emission index was measured two to six times, within an interval of a few minutes. The average  $S$ -values are listed in Table 1 (column 8). The listed uncertainty equals the standard deviation of the set of individual measurements; 84% of the measurements have uncertainties smaller than 2%. For a few stars only one measurement is available close to the X-ray observing time. For the relative uncertainty for these single measurement  $S$ -values we have taken 2%, somewhat above the mean relative uncertainty of 1.3% in our sample.

Fig. 1 shows a comparison with previous measurements of  $S$ -values, as listed by Rutten (1987a). The average spread is rather small, about 10%, although individual differences can occur of up to a factor 2. Relatively hot stars, with  $(B - V) < 0.48$  (Fig. 1, top panel), show very little difference (reduced  $\chi^2$  of 0.69) between the measurements presented here and previously obtained measurements, suggesting that the amount of activity of these stars does not vary at a level exceeding the measurement uncertainty on time scales shorter than a few years. For the cooler stars (Fig. 1, bottom panel) the differences are on average much larger (reduced  $\chi^2$  of 9.5).

### 2.2. X-ray data

During the ROSAT All-Sky Survey the satellite scanned the sky in great circles perpendicular to the direction of the Sun. Any particular position on the sky was in the 2° field of view of the Position Sensitive Proportional Counter (PSPC) for about 30 seconds once every 90 minutes, during at least 2 days (depending on the ecliptic latitude). The PSPC is sensitive in the energy range 0.1–2.4 keV. For a detailed description of the satellite and the PSPC we refer to Trümper (1983) and Pfeffermann et al. (1988), and for a description of the All-Sky Survey to Voges (1992).

The X-ray count rates are derived as described in Chapter 2 of Pters (1995), and are given in Table 1 (column 9). We detected 134 X-ray sources out of the total of 215 stars, with the threshold value for detection set such that less than 0.5 false detections are expected. For the stars that were not detected, we derived a  $3\sigma$  upper limit from the total number of counts (as given by the Standard Analysis Software System, SASS; see Voges 1992, and Voges et al. 1992). These upper limits are also given in Table 1 (column 9).

There appears to be a systematic offset in the count rates determined in this paper and in a paper by Hempelmann et al. (1996); the latter are higher by about 30%. This difference is as yet not fully understood, but may be related to the exposure time corrections derived by the SASS, and used in the

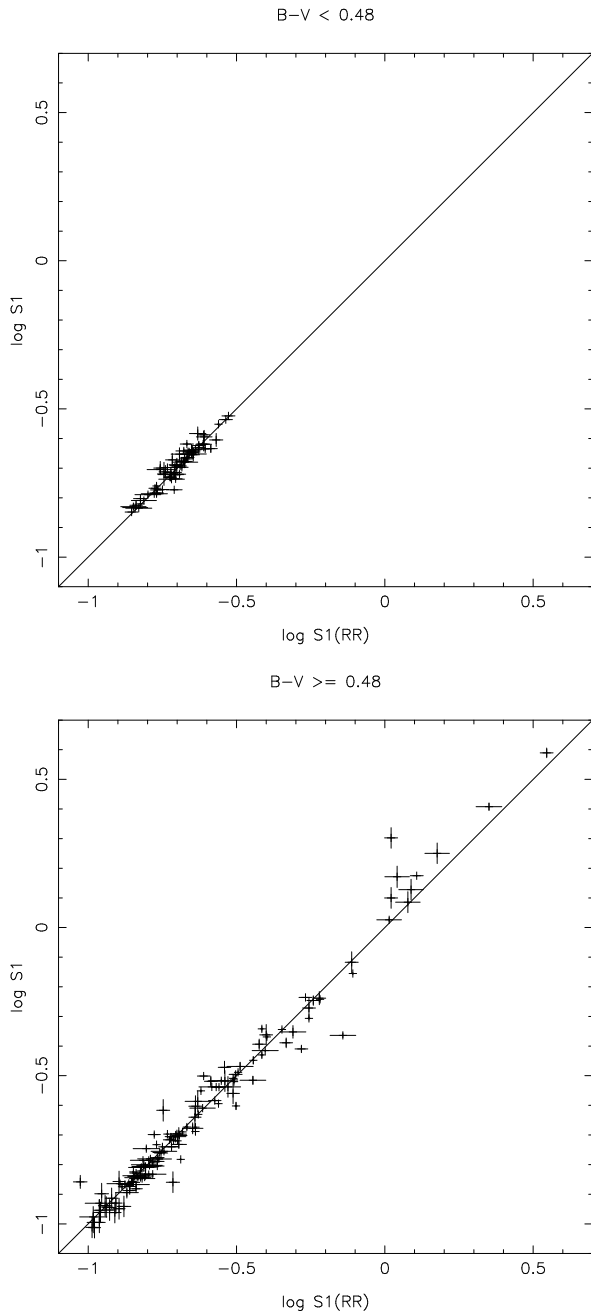


**Fig. 1.** The  $S_1$  values derived here vs. the ones listed by Rutten (1987a). Top:  $(B - V) < 0.48$ ; bottom:  $(B - V) \geq 0.48$ .

paper by Hempelmann et al. (1996). We stress that a constant normalisation factor that would have to be applied in case the offset is caused by an error on our part does not affect any of the conclusions reached in this paper, as it affects only the constant of proportionality in the fits.

The conversion of count rate to flux density at Earth  $f_X$  is given by

$$f_X = \frac{r_s}{C_X} \quad (1)$$

where  $C_X$  is the energy-conversion factor, derived from the ROSAT hardness ratio  $h$  and from the hydrogen column density  $N_H$ , following the method described in PETERS (1995; Ch. 2). The hardness ratio and its uncertainty are listed in column 10 of Table 1. For nearby stars in the galactic plane (distance less than 200 pc and galactic latitude between  $-30^\circ$  and  $+30^\circ$ ) we derived  $N_H$  from Paresce (1984), while for more distant stars we estimated  $N_H$  from the interstellar reddening  $E(B - V)$  using the expression  $N_H = 5.8 \cdot 10^{21} E(B - V) \text{ cm}^{-2}$  (Bohlin et al. 1978). The spread around this relationship is about 30%. The adopted  $N_H$  values are listed in Table 1, column 11. The distance is derived from the parallax or, if the parallax is not known, from the distance modulus, using the absolute magnitudes listed by Schmidt-Kaler (1982).

The ROSAT hardness ratio used here is defined as the ratio between the source count rate in PSPC channels 41–240 ( $\sim 0.4$ – $2.4$  keV) and the total source count rate. The hardness of the soft X-ray spectrum is a measure for the mean coronal temperature. The hardness ratio increases with temperature up to 5 MK, and then decreases slightly for higher temperatures (see Chapter 2 of PETERS, 1995). For spectra with only a few counts, this hardness ratio can still yield valuable information about the coronal temperature structure, provided that the column density is known: for high values of the column density the number of counts in the low-energy band is suppressed, and consequently the hardness ratio is higher.

For the main-sequence stars in our sample we see a strong correlation of hardness ratio with the X-ray surface flux density (Fig. 2, top; the derivation of the surface flux density is described in the next section), suggesting (see Schrijver et al., 1987) that as a star becomes more active, it will either heat up the coronal material as a whole or produce more high-temperature plasma. Both options have the effect of increasing the hardness ratio of the spectrum. For giants this trend is somewhat less pronounced (Fig. 2, bottom).

Note that since the countrate-to-flux conversion factor  $C_X$  depends on the hardness ratio, it depends on the X-ray flux density itself! Not taking into account this dependence (for simplicity, the coronal temperature structure is usually assumed to be the same for all stars) would therefore affect the slope of the flux-flux relationships, as discussed in Section 5.2.

### 3. Stellar surface flux densities

#### 3.1. Ca II H&K flux densities

The surface flux density in the cores of the Ca II H&K lines,  $F_{\text{CaII}}$ , has been derived from the  $S$ -values following Rutten (1984), using his ‘arbitrary’ units:

$$F_{\text{CaII}} = 10^{-14} S C_{\text{cf}} T_{\text{eff}}^4 \quad (2)$$

where the conversion factor  $C_{\text{cf}}$  depends on  $(B - V)$  and luminosity class (Rutten 1984), and  $T_{\text{eff}}$  has been taken from Flower (1977) for giants with  $(B - V) < 0.90$ , and from Böhm-Vitense (1981) for all other stars.

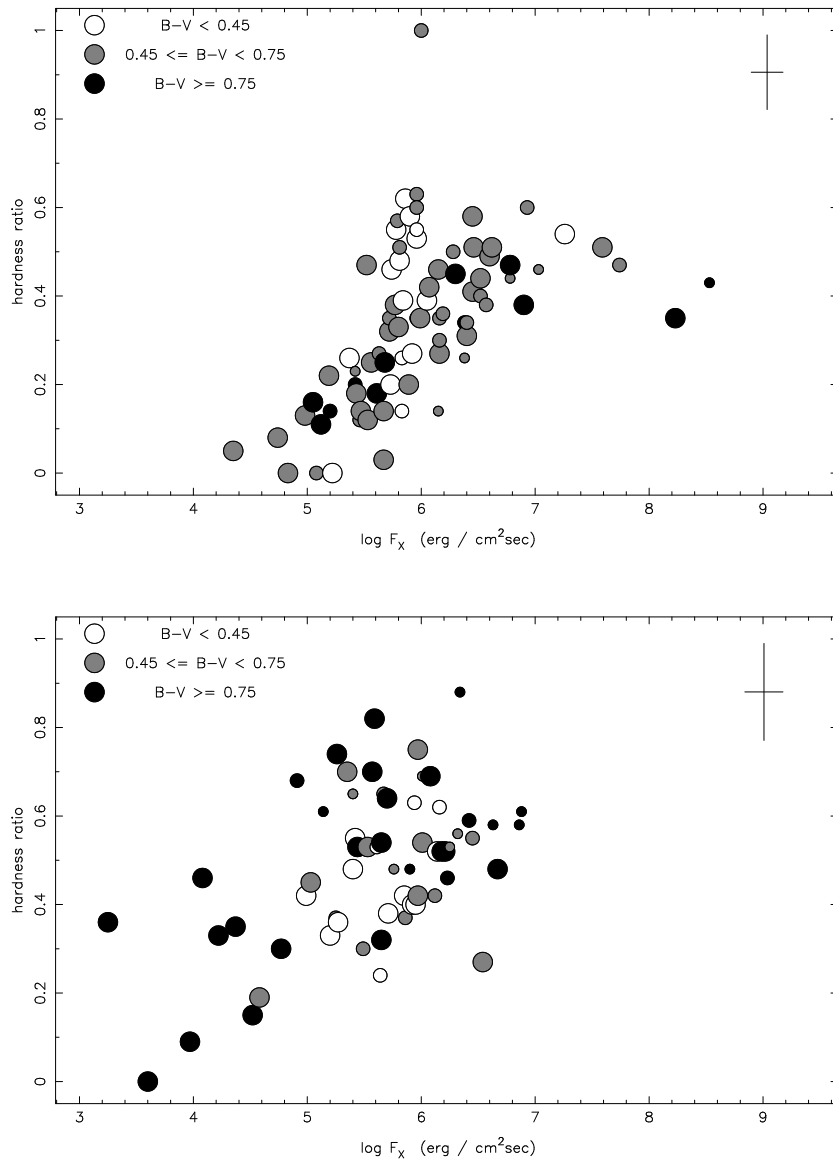


**Fig. 2.** Hardness ratio as a function of X-ray surface flux density for main-sequence stars (LC IV-V and V) (top) and giants (LC IV and up) (bottom). Stars with hydrogen column density  $N_{\text{H}} > 10^{20}$  are indicated by small circles. The average uncertainty is indicated by the cross in the upper right corner.

The flux density in the Ca II line cores only partially originates in the active chromosphere. The other part, the so-called *minimum flux*, is of photospheric (line wings) and of basal (possibly acoustic) origin (see, e.g., Schrijver 1987). By subtracting this (colour-dependent) minimum flux component, we derive the *excess flux density*, which is listed in Table 2, column 2. For this minimum flux we have used the empirical minimum flux derived by Rutten (1987b), for a large sample of stars with luminosity classes between II-III and V. Rutten (1986) shows that this minimum flux is similar to the sum of two theoretically expected contributions: a line-wing contribution, and a minimum line-core contribution, both depending predominantly on effective temperature. Therefore, the minimum flux is taken the same for dwarfs and giants, in spite of the fact that the lowest observed fluxes for dwarfs with  $(B - V) > 1.0$  are higher than this minimum flux.

The minimum flux is given for the  $1\text{\AA}$  passband, so we have converted the  $S_2$ -values to  $S_1$ -values using the relations  $S_1 = \alpha S_2 + \beta$ , where  $\alpha$  and  $\beta$  are given in Table 3 as a function of colour ( $B - V$ ) and luminosity class LC. We have derived these relations from a sample of stars for which both  $S_1$  and  $S_2$  values have been measured (data listed by Rutten 1987a). The scatter  $\sigma$  about the relationships is listed in Table 3; this scatter has been taken into account as an additional uncertainty in the  $S_1$  value, caused by the conversion. The conversion for stars with  $0.50 < (B - V) \leq 0.75$  is only slightly different from the conversion for cooler stars, but still results in a difference of about 20% at the lowest activity levels ( $S_2 \approx 0.3$ ), and after subtraction of the minimum flux density this can lead to large differences in the excess flux density.

The conversion depends on the profile of the line core emission (basal and magnetic) and on the photospheric absorption profile. These profiles depend strongly on colour and luminos-

**Table 3.** Conversion from the  $S_2$  value to the  $S_1$  value using the relation  $S_1 = \alpha S_2 + \beta$ . Listed are  $\alpha$  (left) and  $\beta$  (middle) with their uncertainties (between parentheses). Also listed are the number of data-points  $n$  which define the relationship, and the scatter  $\sigma$  around the relationship.

$(B - V)$	Iab-Ib / IIab	IIb / II-III	III / V
0.20 – 0.50			0.33 0.06 $n = 19$ (0.05) (0.02) $\sigma = 5\%$
0.51 – 0.75			0.69 –0.09 $n = 14$ (0.05) (0.02) $\sigma = 4\%$
0.76 – 0.97		0.65 –0.046 $n = 44$	
0.98 – 1.66	0.42 0.024 $n = 11$	(0.02) (0.008) $\sigma = 8\%$	
1.67 – 1.83	(0.03) (0.011) $\sigma = 5\%$		

ity class, so it is not surprising that we find different relations for the conversion of  $S_2$  to  $S_1$ . However, we do not find a significant difference between the conversion for giants (III) and dwarfs (V). In trying to understand the different relationships, we describe the  $S$ -value as a sum of two different parts: a minimum (photospheric and basal) component and a magnetic emission component. Two stars with different activity levels, but otherwise identical, will only show a difference in the amount of magnetic emission. Both stars have the same relative transmission of the magnetic emission component through the  $1\text{\AA}$  passband, as long as the width of the magnetic emission profile does not change with activity level (which is valid for active regions on the sun, Oranje 1983). The difference between the  $S_1$ -values of both stars is equal to the difference between the  $S_2$ -values scaled with the  $1\text{\AA}$  passband transmission factor and with the ratio of the (constant) normalisation factors of  $S_1$  and  $S_2$ . The slope  $\alpha$  of the relations in Table 3 is the product of these two scaling factors, and not the transmission factor alone, as Schrijver et al. (1992) suggested. Wilson and Bappu (1957) showed that the width of the line core emission peak depends mainly on luminosity: about  $0.5\text{\AA}$  for dwarfs,  $1\text{\AA}$  for giants, and  $2\text{\AA}$  for supergiants. This means that the transmission through the  $1\text{\AA}$  passband is significantly smaller for bright giants than for giants, but the difference between the transmission for giants and dwarfs is not so pronounced, explaining the change in the slope of the conversion relationship around luminosity class II. It is remarkable that relatively cool stars ( $(B - V) > 0.50$ ) appear to have a larger transmission than relatively hot stars. This implies that the width of the line-core emission is much larger (about a factor 2 to 3) for stars with  $(B - V) \leq 0.50$  than for cooler stars. This effect could partly be caused by rotational broadening in the (on average) faster rotating early type stars, which has the effect of moving part of the line-wing contribution to the line core. However, if we divide the sample of stars with colours  $0.20 < (B - V) < 0.75$  in two groups according to their rotational velocities, the change in slope  $\alpha$  is not very significant: the maximum difference in slope occurs between stars with  $v \sin i < 25 \text{ km sec}^{-1}$  ( $\alpha = 0.75 \pm 0.14$ ) and stars with  $v \sin i > 25 \text{ km sec}^{-1}$  ( $\alpha = 0.54 \pm 0.09$ ). Wilson and Bappu (1957) found that the width of the line core emission peak does not depend on effective temperature. However, the stars they used for their study are relatively cool:  $(B - V) > 0.55$ , so

they could not have noticed the dependence we find here. For giants and dwarfs with  $(B - V) > 0.50$  we do not find a change in the slope  $\alpha$  with colour, either, consistent with the findings of Wilson and Bappu (1957).

### 3.2. X-ray flux densities

For each star detected in the ROSAT survey we derived the X-ray flux density at the stellar surface,  $F_X$ , from the flux density on the detector,  $f_X$ , following Oranje et al. (1982):

$$\log F_X = \log f_X + 0.4(V_0 + BC) + 4 \log T_{\text{eff}} + 0.328 . \quad (3)$$

The intrinsic colour index  $(B - V)_0$  is from Fitzgerald (1970), bolometric corrections from Johnson (1966) for dwarfs and from Flower (1977) for giants. The surface flux densities  $F_X$  are listed in Table 2, column 5. The uncertainties in the surface flux densities are dominated by the uncertainties in the source count rate  $r_s$  and in the hydrogen column density  $N_H$ , the latter being caused by the relatively large uncertainties in the distance and in  $E(B - V)$ .

## 4. Relationship between chromospheric and coronal emission

### 4.1. Single stars

Rutten & Schrijver (1987) and Basri (1987) suggested that the *surface flux density*  $F$  is the appropriate unit in which to express the radiative emission measuring magnetic activity level, because the activity-rotation relation is tightest when the activity is expressed in  $F$ , while it strongly depends on luminosity class when the luminosity  $L = 4\pi R^2 F$  is used as an activity unit, and it seems to be slightly colour dependent when the activity is expressed in units of the normalised emission  $R = F/F_{\text{bol}}$ . Rutten and Schrijver (1987) further showed that the flux-flux relations are tightest between surface flux densities and between normalised emissions. These findings can only partly be confirmed here: we show below that the relationship expressed in *normalised emissions* is tightest.

We study the relation between the chromospheric and coronal emission for each of the units (surface flux density  $F$ , normalised emission  $R$  and luminosity  $L$ ). For this purpose we

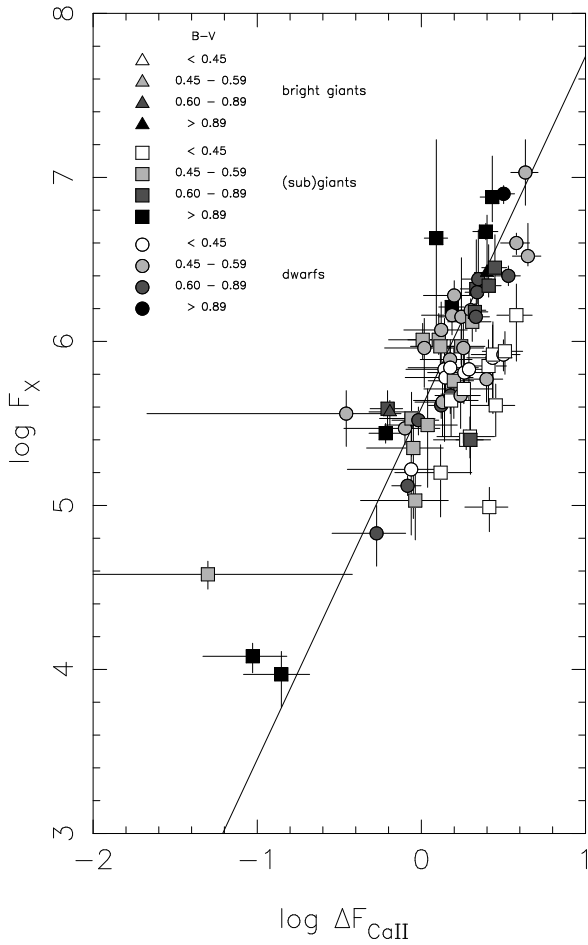


**Fig. 3.** Same as Fig. 3, but for surface flux densities. The solid line represents the best-fit power law relation for stars with  $(B - V) > 0.45$  (see Table 4).

selected the 71 stars from our sample, which are single or single-lined spectroscopic binaries. The latter have been included because we expect that both the observed X-ray flux and the Ca II H&K flux originate in the primary component, the secondary probably being too faint to observe. A power-law fit is determined by minimising  $\chi^2$ , defined as the sum of the quadratic distances to the fit, expressed in units of the individual error ellipses (each term is the square of the factor by which the error ellipse must be multiplied to touch the relation  $y = a + bx$ ):

$$\chi^2 = \sum \frac{(y_i - a - bx_i)^2}{(\sigma_{y_i}^2 + b^2 \sigma_{x_i}^2)} \quad (4)$$

Here  $y_i$  and  $x_i$  are the logarithmic (excess) emissions.

In Figs. 3, 4 and 5 we show logarithmic plots of the ROSAT X-ray emission versus the Ca II H&K line core emission expressed in the three different units, with the best power-law fit (solid line). The results of the fitting procedure are summarised in Table 4, which lists the minimum reduced  $\chi^2$  for every unit and, for  $\chi^2_{\nu} < 1.5$ , the best-fit parameters. The uncertainties in these best-fit parameters have been determined using a ‘bootstrap’ method. In this method we selected 1000 equally large

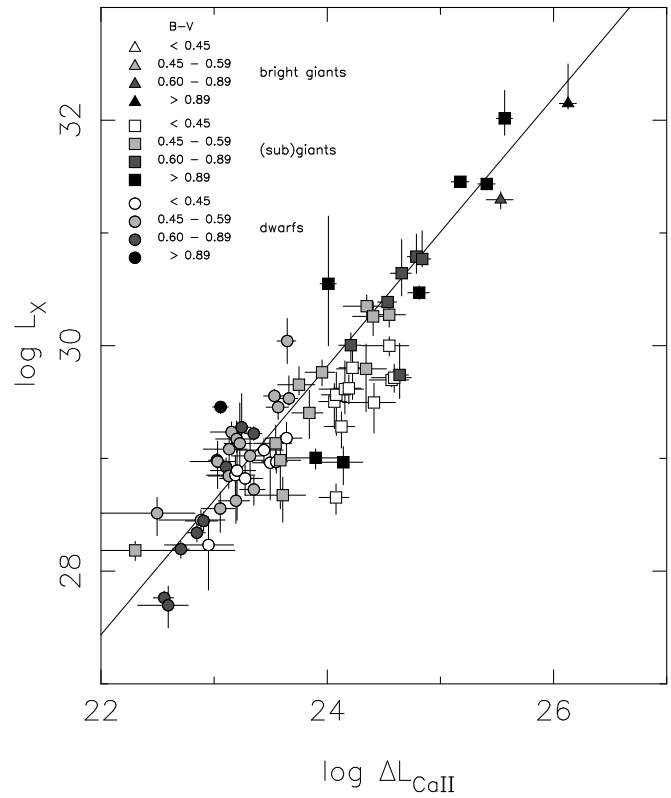


**Fig. 4.** The relationship between ROSAT X-ray luminosity and Mt. Wilson Ca II H&K line core excess luminosity for single stars and single-lined spectroscopic binaries. The solid line represents the ‘best-fit’ power law, with  $\chi^2_{\nu} = 3.7$ .

**Table 4.** The minimum reduced  $\chi^2$  for the flux-flux relationship between different units of radiative emission, and the fitting parameters  $a$  and  $b$ , where  $y = a + bx$  ( $y$  being the X-ray emission, and  $x$  the Ca II emission).

unit	$\chi^2_{\nu}$	$a$	$b$
luminosity $L$	3.7		
surface flux density $F$	1.6		
$F$ , excluding stars			
with $B - V < 0.45$	1.1	$5.60 \pm 0.08$	$2.1 \pm 0.2$
normalised emission $R$	1.04	$17.8 \pm 1.4$	$2.14 \pm 0.14$

random sets of data points from our sample, allowing duplications. We then determined the best fit for each set by minimising  $\chi^2$ . The uncertainties in the parameters are given by the standard deviations.

We confirm the findings of Rutten and Schrijver (1987) that no tight relation exists between  $L_X$  and  $\Delta L_{\text{CaII}}$ . The reduced  $\chi^2$  of the best power-law fit is 3.7, and is therefore unacceptable.

Also the best power-law fit for the surface flux densities, with a reduced  $\chi^2$  of 1.6, is unacceptable: if we assume that the data follow a power-law relation and have normally distributed errors, the probability of finding a reduced  $\chi^2 \geq 1.6$ , for 71 data points and two fit parameters, is 0.11%.

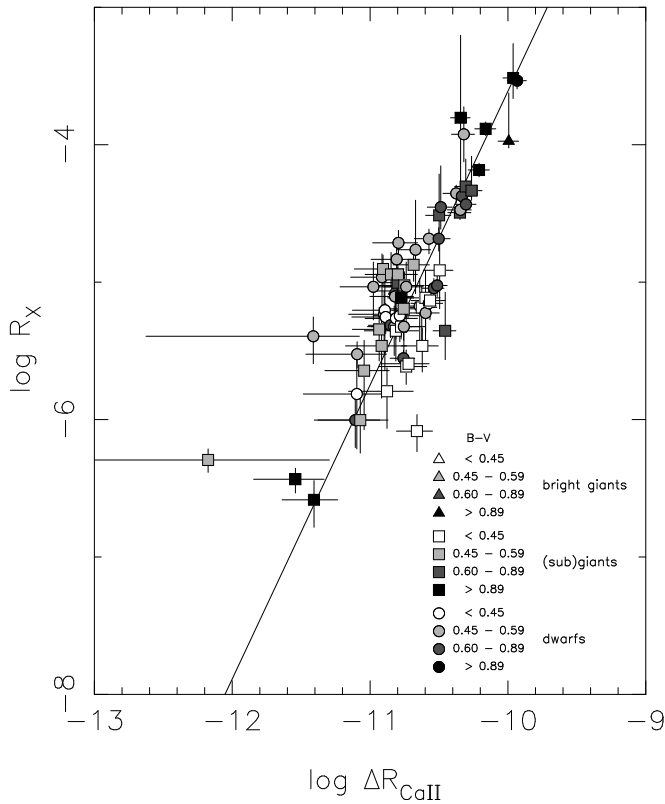


**Fig. 5.** Same as Fig. 3, but for normalised emissions  $R = F/F_{\text{bol}}$ . The solid line represents the best-fit power law (see Table 4).

However, if we exclude the 19 stars with  $(B - V) < 0.45$ , (spectral types between F0 and F4), we find an acceptable power-law fit for the surface flux densities, with a reduced  $\chi^2$  of 1.1; the probability of finding a reduced  $\chi^2 \geq 1.1$  (52 data points) is 20%. Since Rutten and Schrijver (1987) based their results on a sample which contained very few warm stars, this might explain why they found an acceptable power-law fit for the relation between surface flux densities. The slope ( $b$ ) of the relation is larger than the one derived by Schrijver et al. (1992) who found a slope of  $1.5 \pm 0.2$  for a sample of 20 stars observed with EXOSAT. We discuss this in Sect. 5.2.

Fig. 6 shows the deviation from the relationship between the surface flux densities (top) and the normalised flux densities (bottom) as a function of colour. The rank correlation coefficients *Kendall's*  $\tau$  (Kendall 1975) between the deviation from the relationship and  $(B - V)$  are 0.42 and 0.07, respectively. The probability that  $|\tau|$  exceeds 0.07, for 71 non-correlated data points, is 40%, but the probability that it exceeds 0.42 is  $1.8 \cdot 10^{-7}$ . We therefore conclude that the relation between normalised emission units is much less colour dependent than the relation between surface flux densities (which is already suggested by the value of  $\chi^2$  for normalised emission, which is very close to 1; see Table 4), although there may be a weak dependence on colour for  $(B - V) < 0.55$ . Thus, on the basis of our extensive data set, it appears that the normalised emission units provide a better measure of magnetic activity than the surface

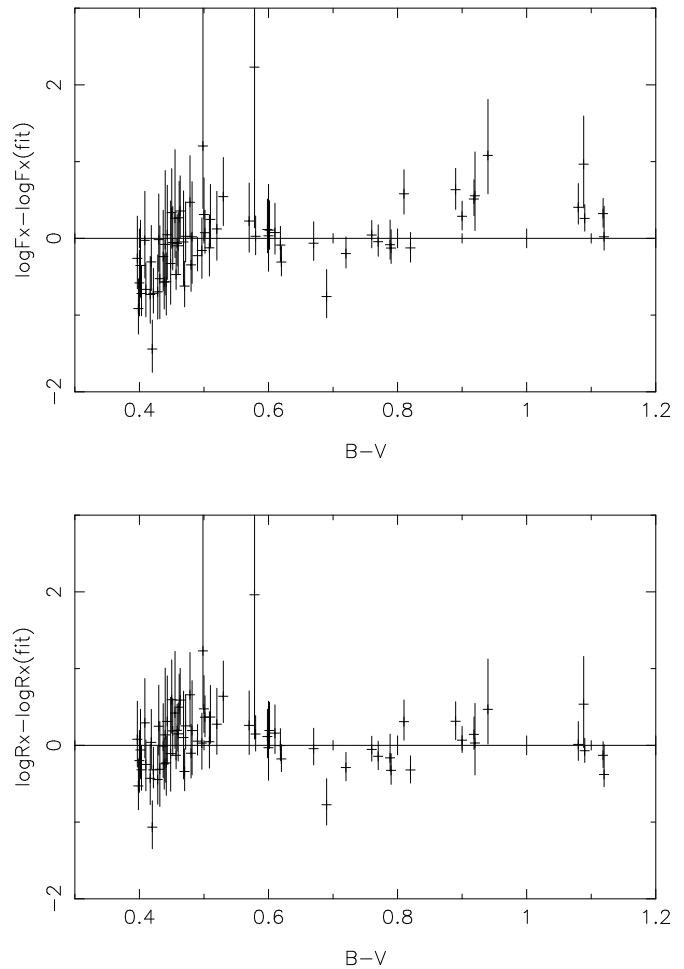


**Fig. 6.** Top: Deviation from the best fit power-law relation (for stars with  $(B - V) > 0.45$ ) between  $F_X$  and  $\Delta F_{\text{CaII}}$  expressed in units of  $\log F_X(\text{obs}) - \log F_X(\text{fit})$  as a function of  $(B - V)$ . Bottom: The deviation from the best fit power-law relation (including stars with  $(B - V) < 0.45$ ) between normalised emissions expressed in units of  $\log R_X(\text{obs}) - \log R_X(\text{fit})$  as a function of  $(B - V)$ . Stars with the same  $(B - V)$  have been separated by an amount 0.0016 in  $(B - V)$  with respect to each other, in order to be able to distinguish individual stars.

flux densities, when comparing radiative emission measures in different temperature regimes.

For the 79 stars that were not detected with ROSAT, we have derived  $3\sigma$  upper limit values to the normalised X-ray emission, as described in Piter's (1995). These values are shown in Fig. 7 (top panel). Given the number of stars, essentially none of them would be expected to have a higher flux than the given upper limit, so that the upper limits should all lie above the mean relationship. Five stars, however, lie below the mean relationship. We attribute this to the uncertainty in the Ca II flux: for these 79 stars we expect about 16%, or 13 stars, to have a Ca II flux density value that exceeds the actual value by more than its one  $\sigma$  uncertainty, and 3%, or two stars, with an

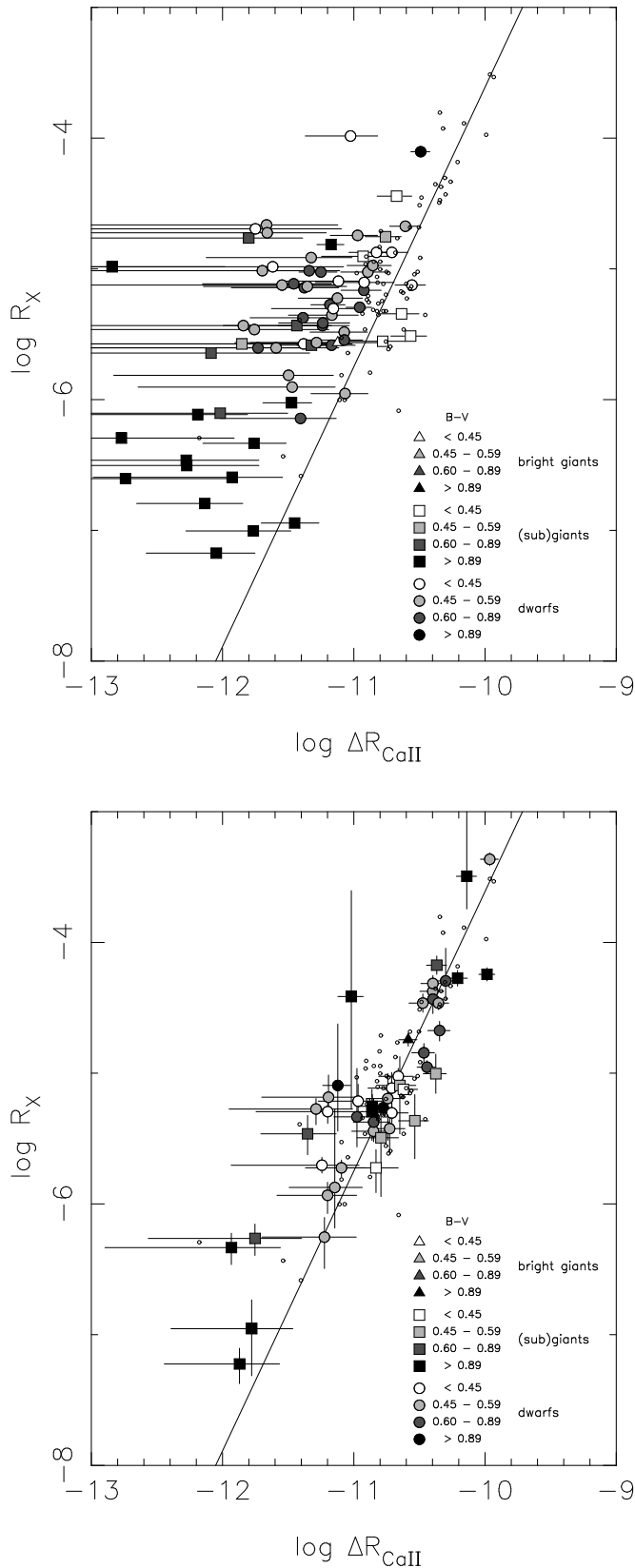


**Fig. 7.** Same as Fig. 5, but now for specific groups of stars. The smallest circles repeat the positions of the stars from Fig. 5, which define the best-fit relationship between normalised emissions (solid line). Top: stars with only upper limits in  $R_X$ ; bottom: binary stars.

observed flux density too high by more than  $2\sigma$ . This appears consistent with our data.

#### 4.2. Binaries

The flux-flux diagram for visual binaries (with a distance of less than  $100''$ ) and double-lined spectroscopic binaries is shown in Fig. 7 (bottom panel). The calculation of the normalised flux density is the same as for the single stars (Sect. 3), where we used the stellar parameters of the primary component. On average, these binaries follow the relationship defined by the single stars, but the spread is substantially larger than for single stars ( $\chi^2_\nu = 1.7$ ). We attribute this scatter to contributions from the secondaries, both in X-rays and in Ca II H&K. In the simple case of two identical stars with the same magnetic activity level, for instance, we would expect the binary system, analysed as if it were a single star, to lie a factor 2 above the relationship, because the  $S$ -value is the same as for one star, while the X-ray count rate is twice as high as for one star.

#### 4.3. The effect of variability

Stellar magnetic activity is intrinsically variable. The effect of this variability on the  $S$ -value for stars with  $(B-V) \geq 0.48$  can be seen in Fig. 1 (bottom panel). We investigate the effect of the time difference between the observing times in X-ray and Ca II on the scatter about the relationship between the normalised emissions. There is no significant correlation between the distance to the relationship (i.e.  $|\log R_X(\text{obs}) - \log R_X(\text{fit})|$ ) and the time difference between the X-ray and the Ca II H&K measurements, for stars with  $(B-V) \geq 0.48$  and  $R_X$  between  $10^{-4}$  and  $10^{-6}$  (nor between the distance and the time difference normalised to the rotation period). The X-ray measurements are averages over time intervals of at least two days (Sect. 2.2), so we do not expect to detect variations from the relationship due to variations in activity level on time scales smaller than two days. If we exclude stars which have been observed more than two days apart in X-ray and in Ca II in deriving the relationship between normalised emission units, the reduced  $\chi^2$  for the new relationship between  $R_X$  and  $\Delta R_{CaII}$  with 39 stars becomes 0.94, which is not significantly better than the reduced  $\chi^2$  of 1.04 derived for 71 stars (see Table 4). We conclude from this that deviations from the relationship due to variations in activity level on time scales of a few days are of the same order as or less than the observational uncertainties due to statistical effects and calibrations.

The root mean square of the (logarithmic) differences between the observed X-ray emission and the value expected from the fitted relationship equals 0.43, i.e., somewhat larger than that derived by Schrijver (1983; scatter is 0.35). This is mainly caused by the relatively large uncertainties in the ROSAT All-Sky Survey fluxes as compared to those obtained from the Einstein observations used by Schrijver (1983). We note, however, that in deriving the best fit relationship we minimised  $\chi^2$ , not the above defined scatter. If we include only stars with small observational uncertainties we find that the dispersion around

the relationship is reduced (i.e., to 0.30 for the 38 stars with uncertainties in (logarithmic) X-ray and Ca II emission less than 0.3 and 0.15, respectively, and to 0.20 for the 20 stars with uncertainties in X-ray and Ca II emission less than 0.2 and 0.1, respectively). This shows that independent of the observational uncertainties, the dispersion around the average relation is largely accounted for by these uncertainties.

## 5. Discussion

### 5.1. The appropriate magnetic-activity unit

We argued in Sect. 4.1 that in comparing chromospheric and coronal emissions, the normalised emission  $R$  provides a better measure of magnetic activity than the surface flux density  $F$ , because the relationship between the normalised emission units is valid in the complete colour range  $0.4 \leq (B - V) \leq 1.1$  investigated here, while the relationship between surface flux densities is only valid for stars with  $(B - V) \geq 0.45$ . Rutten et al. (1991) and Schrijver et al. (1992) found a good relationship between surface flux densities, because the sample they used consisted mainly of stars with  $(B - V) > 0.6$ . Note, however, that in this paper we do not consider the dependence of the emissions on stellar rotation rate, whereas Basri (1987) and Rutten and Schrijver (1987) based their preference for the surface flux density  $F$  as the most appropriate measure of magnetic activity largely on the basis of the relation between chromospheric activity and stellar rotation rate.

Some authors state that relations between normalised emission from the corona and the chromosphere/transition region are colour dependent, in contradiction with our results. Simon and Drake (1989) find, that early F stars lie systematically below the relation between normalised emission of coronal X-rays and of the transition region C IV line. This deviation can be attributed to the minimum flux contribution of the C IV line (Rutten et al. 1991), which the authors did not subtract from the normalised emission. The minimum emission for early F stars is about a factor 200 higher than for K stars. Subtraction of the minimum emission moves the early F stars onto the relationship (Schrijver 1993). Rutten and Schrijver (1987) state that the relationship between normalised emission of X-rays and of the chromospheric Mg II line in excess of the minimum emission is slightly colour dependent, while the relationship between the surface flux densities is not. This statement is based on their Fig. 1, but the colour dependence of the relationship between normalised emission units is not very obvious from this figure, and seems to be based on only three stars with  $(B - V) < 0.6$ , which lie slightly above the mean relation.

### 5.2. The slope of the CaII – X-ray relationship

The relationship between the X-ray surface flux density and the excess Ca II H&K line core excess flux density, as derived from the present data, is steeper than the relation previously found from EXOSAT observations (slope  $1.5 \pm 0.2$ ; Schrijver et al. 1992), and has about the same slope as the relation found by Rutten et al. (1991; slope 1.9) on the basis of Einstein IPC

data. This is probably caused by a combination of two effects. The first one is that Schrijver et al. (1992) derived their relationship giving the same weights to every data point, while here and in Rutten et al. (1991) the points are weighted according to their uncertainties, thereby giving the stars with lowest activity (hence larger uncertainties) less weight. The least active stars — both in the sample used by Schrijver et al. (1992) and in the sample presented here — appear to lie slightly above the relationship so that they lower the slope of the relationship, when given more weight. If we would have derived a relationship with equal uncertainties for all stars in our sample, we would have found a slope of  $1.8 \pm 0.3$  for the relation between surface flux densities  $F$  ( $(B - V) \geq 0.45$ ) and a slope of  $1.9 \pm 0.2$  for the relation between normalised flux densities  $R$ .

The second cause for the higher slope is that constant factors were assumed in the conversion from count rate to flux for the EXOSAT and Einstein data, which is only correct for stars with coronal temperatures higher than a few MK (see Fig. 3a in Schrijver et al. 1992). Fig. 2 (top) shows that the ROSAT hardness ratio tends to increase with the X-ray surface flux density for main-sequence stars, which points to an increase in the average coronal temperature with increasing activity (also observed for IPC data, e.g., Fig. 13 in Vaiana 1983). The use of the same conversion factor for all stars would lead to a relative overestimation of the X-ray flux density of the least active stars, because from a few MK to 1 MK the count-rate-to-flux conversion factor of EXOSAT drops a factor ranging from 2 to 10 (for the 3-Lex filter and the A1/P filter respectively; Fig. 3a in Schrijver et al. 1992). Such an overestimation of the lowest flux densities results in a less steep  $F_X - \Delta F_{\text{CaII}}$  relationship. Using a constant energy conversion factor in the derivation of the relationship for ROSAT data for our sample, we find a slope of  $1.6 \pm 0.3$  for the relation between surface flux densities (equal weights for all stars), consistent with the results of Schrijver et al. (1992), and a slope of  $1.7 \pm 0.2$  for the normalised flux densities.

Our assumption of a one-temperature plasma could, in principle, affect the slope of the  $F_X - \Delta F_{\text{CaII}}$  relationship as well. In calculating the energy conversion factor  $C_X$ , we have assumed that the X-ray emitting plasma is dominated by one temperature, so that the hardness of the spectrum can easily be associated with a temperature and consequently with an energy conversion factor (Sect. 2.2). We investigated the effect of this assumption on the  $C_X$  corresponding to, e.g., a two-temperature plasma, in the following way. For a grid of temperature combinations between  $10^5$  K and  $10^8$  K, we calculated the relative emission measures of the two temperature components for a given hardness ratio, and the corresponding energy conversion factor. We find that even for extreme temperature combinations, this ratio stays close to 1, as long as the hardness ratio is larger than 0.2, which is the case for the large majority of the stars in our sample. For smaller hardness ratios there exist temperature combinations (with temperatures  $T_1 > 2$  MK,  $T_2 < 0.3$  MK and the ratio of the emission measures  $EM_2/EM_1 > 30$ ) such that for the same hardness ratio the one-temperature conversion factor is larger than 1.5 times the two-temperature conversion factor. In this case the calculated X-ray surface flux density (as-

suming one temperature) is underestimated by more than a factor 1.5. If we exclude the 9 stars with hardness ratios smaller than 0.2, the slope of the relationship between surface flux densities becomes  $1.9 \pm 0.2$ , and the slope of the relationship between normalised flux densities becomes  $2.08 \pm 0.17$ , which are not significantly different from the slopes derived for the surface flux densities (for  $(B - V) > 0.45$ ) and the normalised flux densities, respectively.

## 6. Conclusions

For single stars and single-lined spectroscopic binaries a unique relation exists (Table 4 and Fig. 5) between the chromospheric Ca II H&K line-core emission in excess of the minimum emission and the coronal soft X-ray emission, both normalised to the bolometric emission. This relation is approximately quadratic, with power-law exponent  $2.14 \pm 0.14$ , and does not depend on luminosity class or effective temperature within the extremes contained in our present sample. The reduced  $\chi^2$  for this relation is 1.04.

The surface flux densities in X-ray and Ca II define also a unique relation with a reduced  $\chi^2$  of 1.1 (Fig. 4), but only if stars with  $(B - V) \leq 0.45$  are excluded. We conclude therefore that the normalised emission is a more appropriate unit in which to express magnetic activity, when only comparing radiative emission measures, because the relationship between these units is independent of effective temperature.

The reduced  $\chi^2$  for the relationship between normalised emission units is virtually equal to unity, meaning that the scatter about this relationship is dominated by measurement uncertainties. This is also the case if we select stars for which the observational data are most accurately determined. We cannot, therefore, make any statement about the possibility that deviations from this relationship significantly depend on any other parameter, like rotation, effective temperature, or luminosity class.

A strong correlation is seen between the ROSAT hardness ratio and the X-ray surface flux density of main-sequence stars. This suggests that as a star becomes more active, it will either raise the temperature of the coronal material as a whole or produce more high-temperature plasma. Both options have the effect of increasing the hardness ratio of the spectrum. For giants this correlation is less pronounced.

*Acknowledgements.* This research has made use of the SIMBAD database, operated at CDS, Strasbourg, France. C.J. Schrijver acknowledges support by the Royal Netherlands Academy of Arts & Sciences (KNAW). The ROSAT All-Sky Survey data result from the hardware and software efforts of many people in the ROSAT team at MPE. It is a pleasure to acknowledge their dedicated work and continuing support. We gratefully thank J. Frazer and L. Woodard, who have worked very hard to obtain the Mt. Wilson data as simultaneously as possible with the ROSAT observations.

## References

Basri, 1987, ApJ 316, 377

- Bohlin R.C., Savage B.D., Drake J.F., 1978, ApJ 224, 132  
 Böhm-Vitense E., 1981, ARAA 19, 295  
 Fitzgerald M.P., 1970, A&A 4, 234  
 Flower P.J., 1977, A&A 54, 31  
 Hempelmann A., Schmitt J.H.M.M., Stepien K., 1996, A&A 305, 284  
 Johnson H.L., 1966, ARAA 4, 193  
 Kendall, M.G., 1975, Rank Correlation Methods, 5th edition, Griffin, London  
 Oranje B.J., Zwaan C., Middelkoop F., 1982, A&A 110, 30  
 Oranje B.J., 1983, A&A 124, 43  
 Paresce, 1984, AJ 89, 1022  
 Pfeffermann E, Briel U.G., Hippmann H., Kettenring G., Metzner G., Predehl P, Reger G., Stephan K.H., Zombeck M.V., Chappell J., Murray S.S., 1988, Proc. SPIE, Vol. 733, 519  
 PETERS A.J.M., 1995, Ph. D. thesis, University of Amsterdam, The Netherlands  
 Rutten R.G.M., 1984, A&A 130, 353  
 Rutten R.G.M., 1986, A&A 159, 291  
 Rutten R.G.M., 1987a, PhD. thesis, University of Utrecht, The Netherlands  
 Rutten R.G.M., 1987b, A&A 177, 131  
 Rutten R.G.M., Schrijver C.J., 1987, A&A 177, 155  
 Rutten R.G.M., Schrijver C.J., Lemmens A.F.P., Zwaan C., 1991, A&A 252, 203  
 Schmidt-Kaler Th., 1982, in: Landolt-Börnstein: Numerical Data and Functional Relationships in Science and Technology, Scaifers K., Voigt H.H. (eds.), Springer-Verlag, Berlin. Vol. 2b, p. 453 ff.  
 Schrijver C.J., 1983, A&A 127, 289  
 Schrijver C.J., 1987, A&A 172, 111  
 Schrijver C.J., 1991, in "Mechanisms of Chromospheric and Coronal Heating", P. Ulmschneider, E.R. Priest, R.R. Rosner (eds.), Springer-Verlag, Berlin, p. 257  
 Schrijver C.J., 1993, A&A 269, 395  
 Schrijver C.J., Mewe R., Walter F.M., 1987, A&A 138, 258  
 Schrijver C.J., Coté J., Zwaan C., Saar S.H., 1989, ApJ 337, 964  
 Schrijver C.J., Dobson A.K., Radick R.R., 1992, A&A 258, 432  
 Simon T., Drake S.A., 1989, ApJ 346, 303  
 Solanki S.K., Steiner O., Uitenbroek H., 1991, A&A 250, 220  
 Trümper J., 1983, Adv. Space Res., Vol. 2, No. 4, 241  
 Vaiana G.S., 1983, in: Solar and stellar magnetic fields: Origins and coronal effects, Stenflo J.O. (ed.), IAU Symp. 102, Reidel, Dordrecht, p. 165  
 Vaughan A.H., Preston G.W., Wilson O.C., 1978, PASP 90, 267  
 Voges W., 1992, ESA ISY-3, p. 9  
 Voges W., Gruber R., Paul J., Bickert K., Bohnet A., Bursik J., Dennerl K., Englhauser J., Hartner G., Jennert W., Köhler H., Rosso C., 1992, ESA ISY-3, p. 223  
 Wilson O.C., Bappu M.K.V., 1957, ApJ 125, 661  
 Zwaan C., 1991, in: Mechanisms of Chromospheric and Coronal Heating, Ulmschneider P., Priest E., Rosner R. (eds.), Springer-Verlag, p. 241